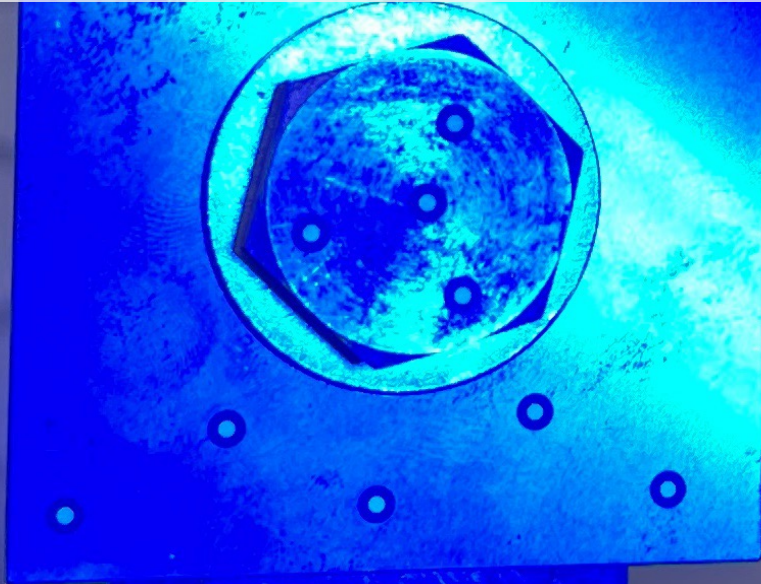


DESIGN, MANUFACTURING, TESTING AND OPTIMIZATION OF BOLT LOADED VARIABLE-AXIAL COMPOSITE LAMINATES



TWENTY-THIRD INTERNATIONAL CONFERENCE ON COMPOSITE MATERIALS (ICCM23)
Belfast | 30th July - 04th August 2023

Axel Spickenheuer^{1,*}, Tales V. Lisbôa¹, E.A.W. de Menezes¹, Markus Stommel^{1,2}, Kai Uhlig¹,
Lars Bittrich¹, Andreas Freund³

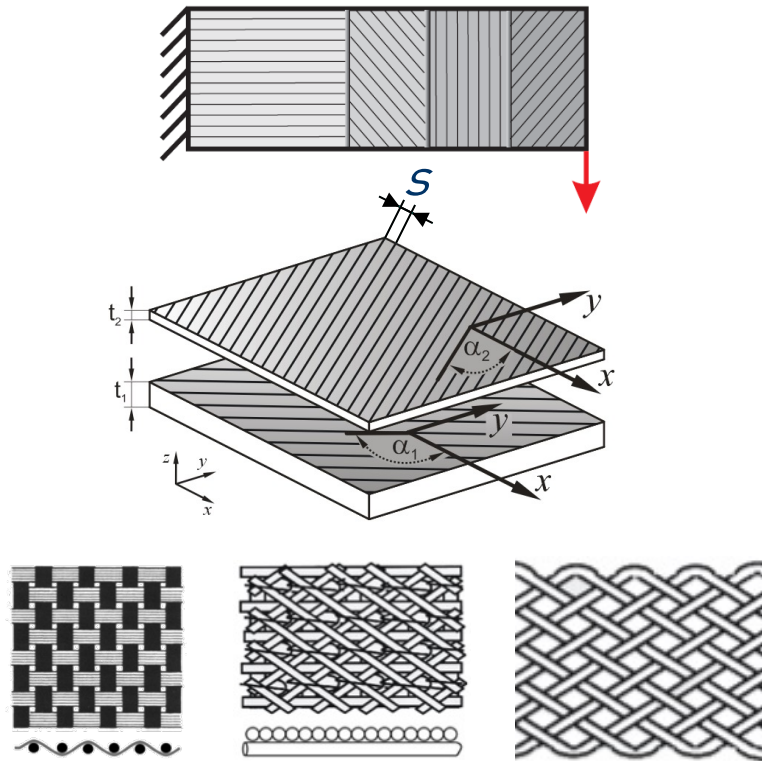
¹ Leibniz-Institute für Polymerforschung Dresden e. V.; ² TU Dresden, Institute of Material Science; ³ Realize Engineering Dresden GmbH



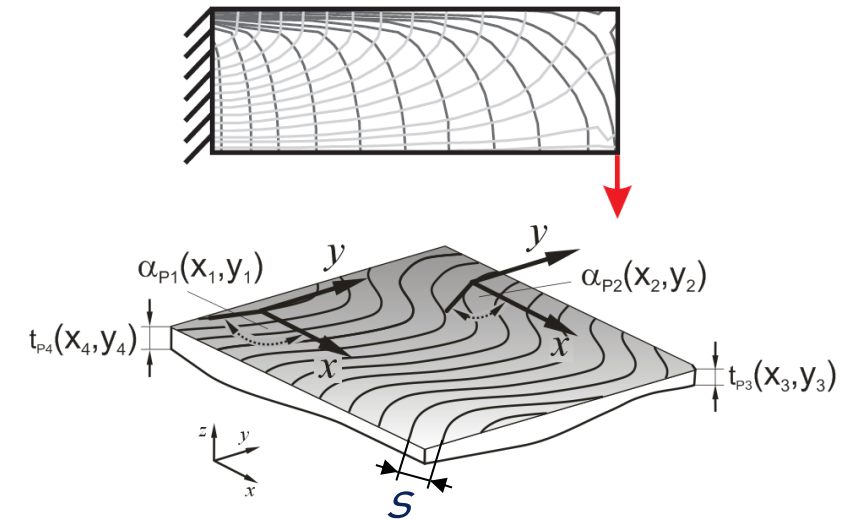
Fiber-reinforced plastics (FRP)

Multi-axial vs. variable-axial

Composite design 1.0 *multi-axial*



Composite design 2.0 *variable-axial*

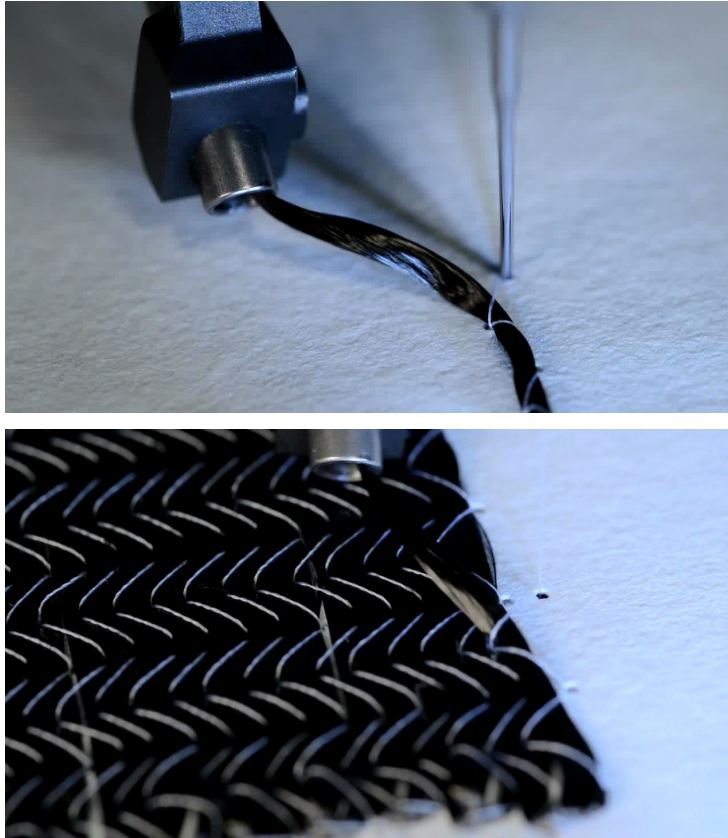


$\alpha \neq \text{const.}$

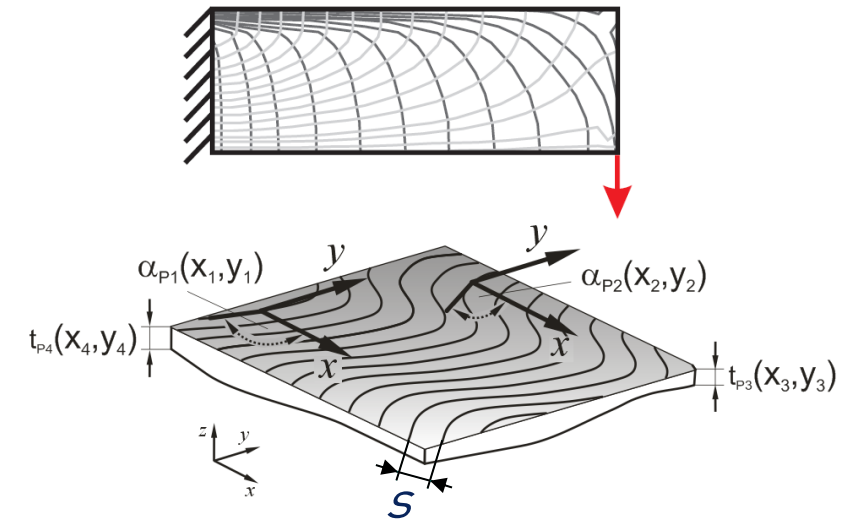
$s \neq \text{const.}$
 $t = f(s)$

Fiber-reinforced plastics (FRP)

Variable-axial FRP by Tailored Fiber Placement (TFP)



Composite design 2.0 *variable-axial*

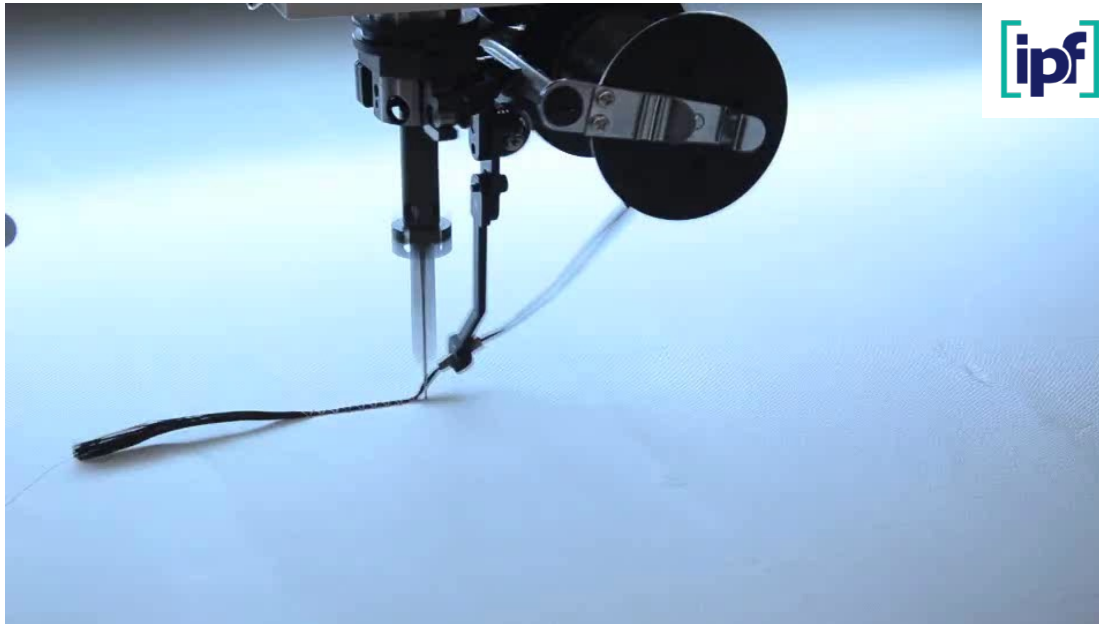


$\alpha \neq \text{const.}$

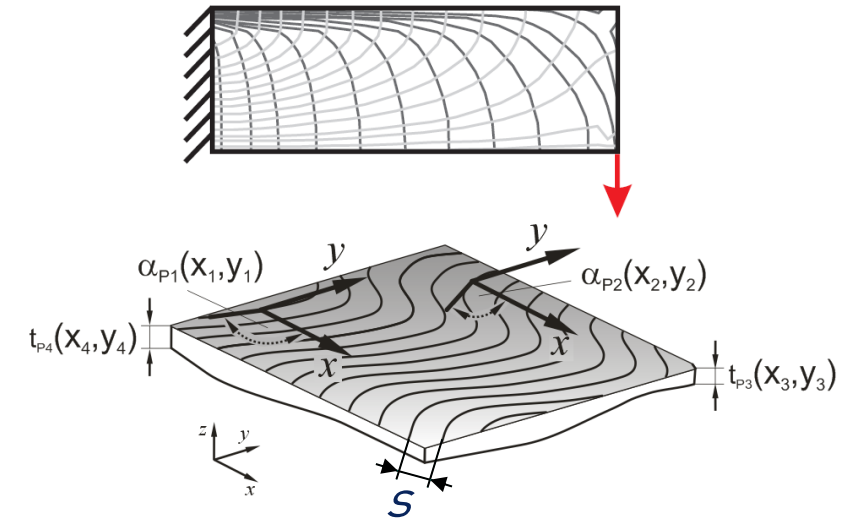
$s \neq \text{const.}$
 $t = f(s)$

Fiber-reinforced plastics (FRP)

Variable-axial FRP by Tailored Fiber Placement (TFP)



Composite design 2.0 *variable-axial*

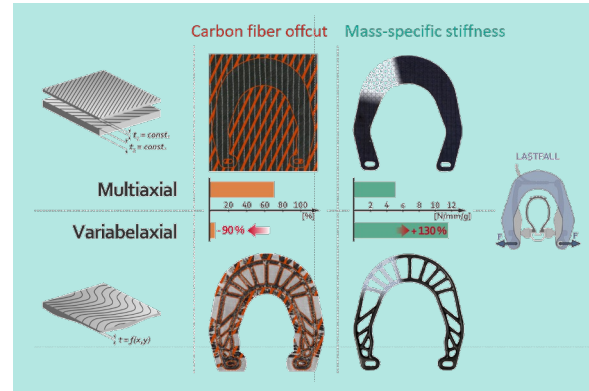
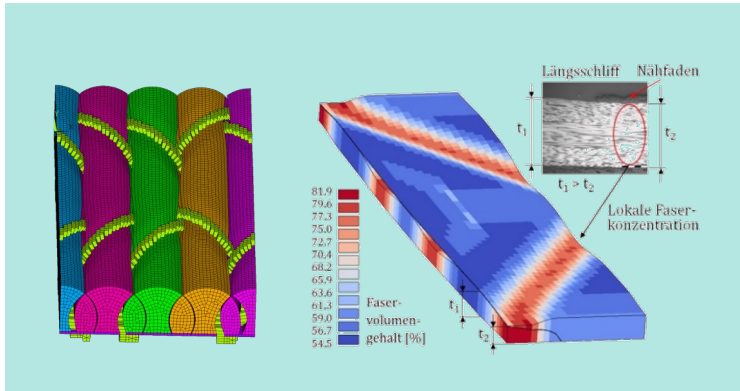


$\alpha \neq \text{const.}$

$s \neq \text{const.}$
 $t = f(s)$

Variable-axial composites made by Tailored Fiber Placement

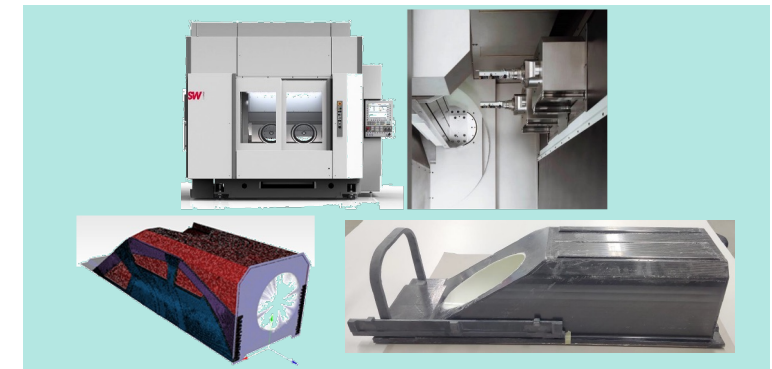
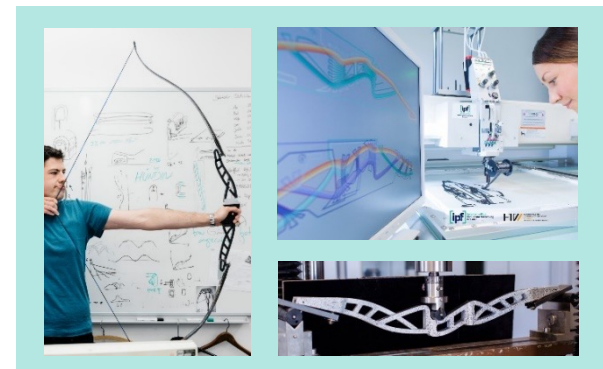
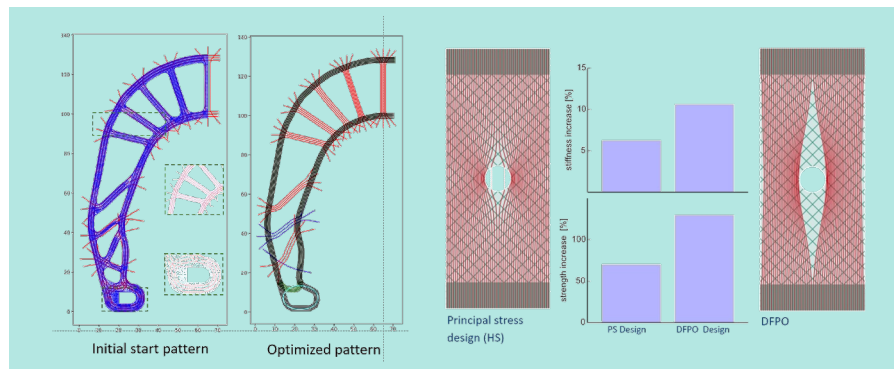
From basic research to industrial deployment



TRL1

TRL4

TRL7

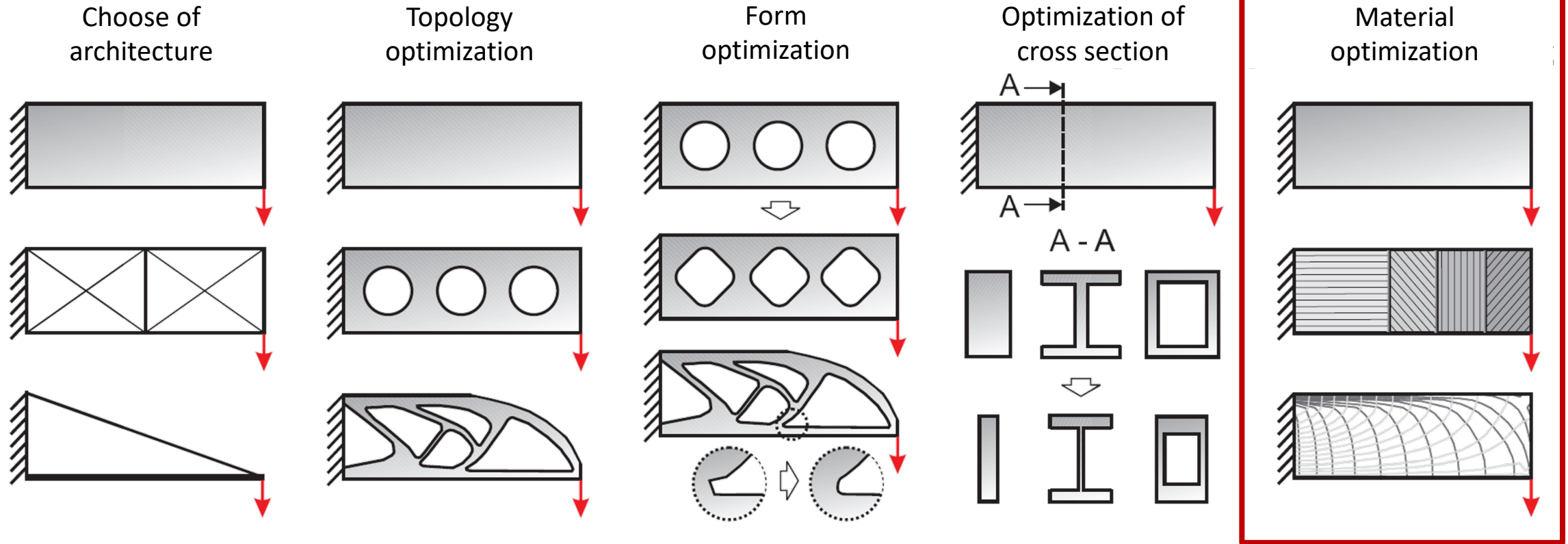


Multi-scale modelling and optimization methods

Process chain for variable-axial composites

Development of industrial components

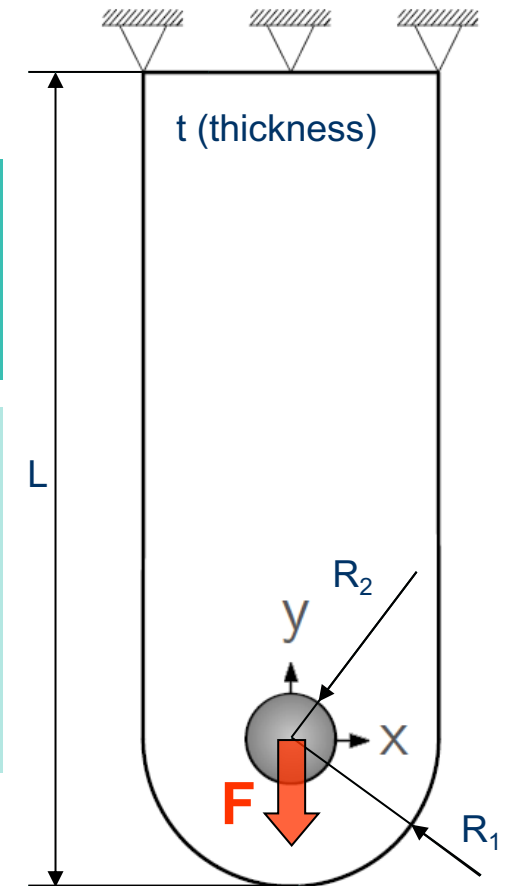
How to design variable-axial composite structures?



Analysis and optimization of bolted joints made by variable-axial laminates

What in-plane fiber orientation strategy shows advantageous mechanical performance?

- Calibration of progressive damage simulation for structural optimization by experimental research
- No consideration of out-of-plane reinforcements



Dimensions of specimen

$R_1 = 25 \text{ mm}$, $R_2 = 7,5 \text{ mm}$,

$L = 170 \text{ mm}$, $t \approx 5 \text{ mm}$

Bolted joints with tailored fiber orientation in literature

1997



PH-S1359-835X(97)00022-5

Composites Part A 28A (1997) 619-625
© 1997 Published by Elsevier Science Limited
Printed in Great Britain. All rights reserved
1359-835X/97/\$17.00

Tailored fibre placement to minimise stress concentrations

P. J. Crothers^{a,*}, K. Drechsler^b, D. Feltn^c, I. Herszberg^a and T. Kruckenberg^d
^aThe Sir Lawrence Wackett Centre for Aerospace Design Technology, Royal Melbourne Institute of Technology, P.O. Box 2476V, Melbourne, Vic. 300, Australia
^bDaimler Benz AG, Research and Technology, P.O. Box 80 04 65, 81663 Munich, Germany
^cInstitute for Polymer Research Dresden (IPF-Dresden), Hohe Straße 6, D-01069 Dresden, Germany
^dCooperative Research Centre for Advanced Composite Structures (CRC-ACS) Ltd, 506 Lorimer St., Fishermans Bend, Vic. 3207, Australia
(Received 16 February 1996; accepted 9 November 1996)

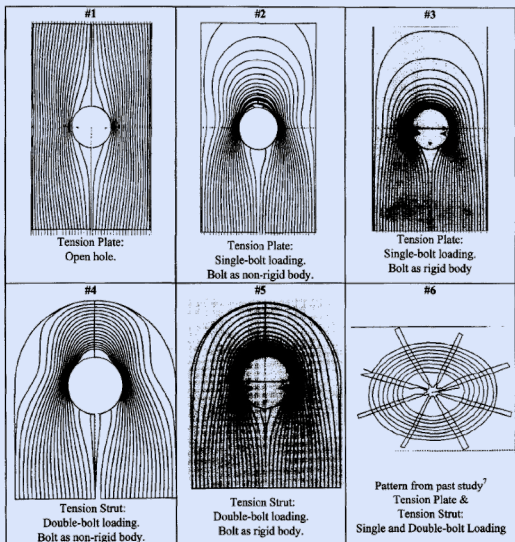


Figure 5. Patterns for TFP reinforcement of test components

1999

Interpreting load paths and stress trajectories in elasticity

D.W. Kelly and M.W. Tosh
School of Mechanical and Manufacturing Engineering,
University of New South Wales, Sydney, Australia

Interpreting load paths

117

Received March 1999
Revised November 1999
Accepted December 1999

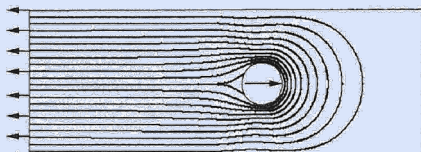


Figure 17.
Major principal stress trajectories (σ_1)

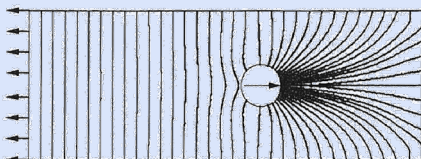


Figure 18.
Minor principal stress trajectories (σ_2)

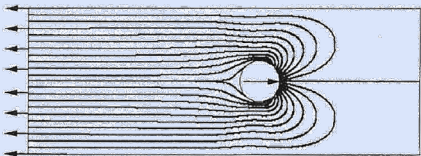
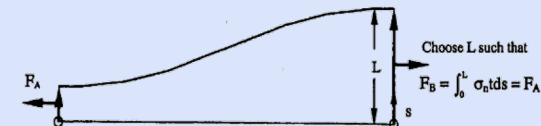


Figure 19.
 F_1 load path contours from the integration technique



2000



Composites: Part A 31 (2000) 1047-1060

composites
Part A: applied science
and manufacturing

www.elsevier.com/locate/compositesa

On the design, manufacture and testing of trajectorial fibre steering for carbon fibre composite laminates^{*}

M.W. Tosh, D.W. Kelly^{*}

School of Mechanical and Manufacturing Engineering, University of New South Wales, Sydney 2052, Australia
Received 7 May 1999; revised 15 March 2000; accepted 23 March 2000

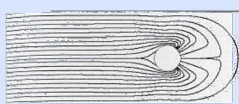


Fig. 15. Contours of dominant principal stress.

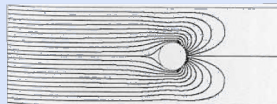


Fig. 16. Dominant or X-direction load paths for an isotropic material.

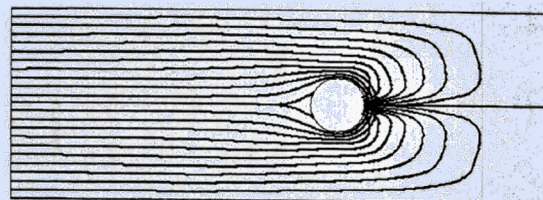
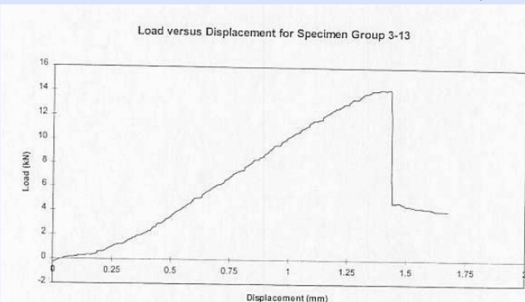


Fig. 21. Hybrid combination of anisotropic load path and tensile principal stress trajectories.



2002



Composite Structures 57 (2002) 377-383

COMPOSITE
STRUCTURES

www.elsevier.com/locate/comstruct

Strength improvement by fibre steering around a pin loaded hole^{*}

R. Li^a, D. Kelly^{a,*}, A. Crosky^b

^aSchool of Mechanical and Manufacturing Engineering, University of New South Wales, Sydney NSW 2052, Australia
^bSchool of Materials Science and Engineering, University of New South Wales, Sydney NSW 2052, Australia

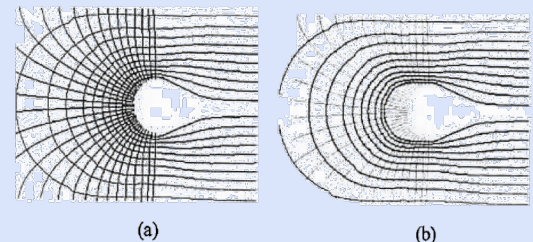


Fig. 9. Reduction of fibre over stacking: (a) FEA pattern; (b) modified pattern.

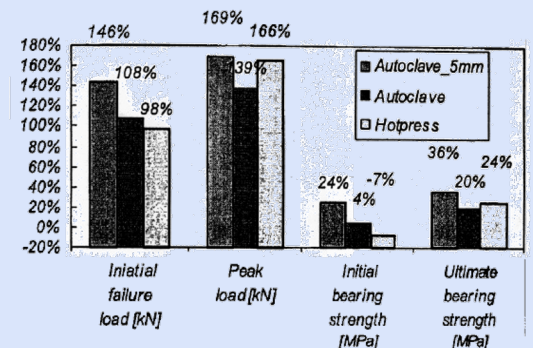


Fig. 10. Effect of fibre steering on strength of the carbon fibre bolted joints.

Bolted joints with tailored fiber orientation in literature

2006

Improving the Efficiency of Fiber Steered Composite Joints using Load Path Trajectories*

R. LI,¹ D. KELLY,^{1,†} A. CROSKY,² H. SCHOEN² AND L. SMOLICH²

¹School of Mechanical and Manufacturing Engineering
University of New South Wales, Sydney 2052, Australia

²School of Materials Science and Engineering
University of New South Wales, Sydney 2052, Australia

(Received February 16, 2005)
(Accepted August 23, 2005)

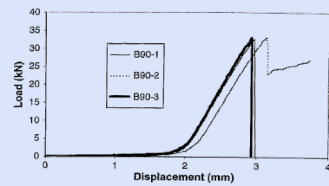


Figure 9. Test curves for 90mm wide baseline specimens.

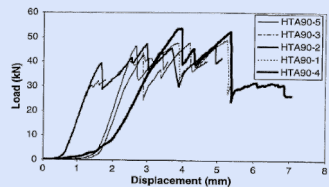


Figure 10. Test curves for 90mm wide steered fiber specimens.

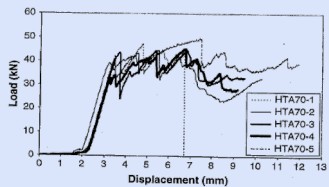


Figure 11. Test curves for 70mm wide steered fiber specimens.

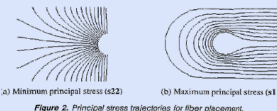


Figure 2. Principal stress trajectories for fiber placement.

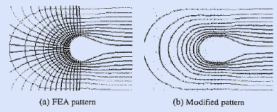


Figure 3. Reduction of fiber over stacking near the bearing surfaces.

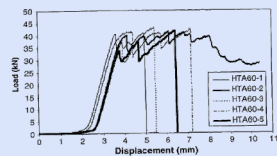


Figure 12. Test curves for 60mm wide steered fiber specimens.

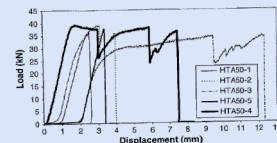


Figure 13. Test curves for 60mm wide steered fiber specimens.

2006



Available online at www.sciencedirect.com
ScienceDirect
Composite Structures 76 (2006) 260–271

COMPOSITE
STRUCTURES

www.elsevier.com/locate/comstruct

Improvement of bearing strength of laminated composites*

A. CROSKY^a, D. KELLY^{b,*}, R. LI^b, X. LEGRAND^c, N. HUONG^a, R. UJJAIN^b

^aSchool of Materials Science and Engineering, University of New South Wales, Sydney, NSW 2052, Australia
^bSchool of Mechanical and Manufacturing Engineering, University of New South Wales, Sydney, NSW 2052, Australia
^cEcole Nationale des Arts et Industries Textiles, Laboratoire GEMTEX, 9 rue de l'Éminage – BP 30329, 59100 Roubaix, France

Available online 1 August 2006

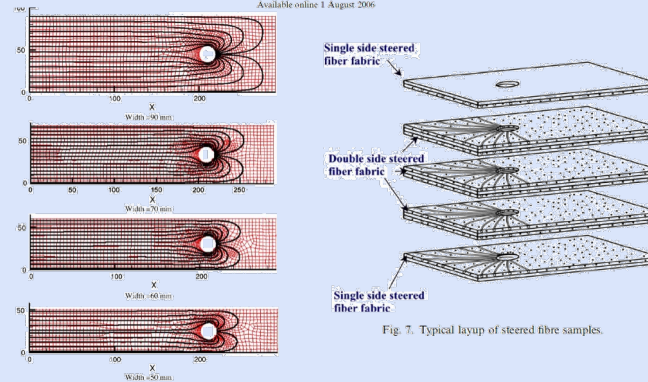


Fig. 7. Typical layout of steered fibre samples.

Fig. 15. Dominant load path trajectories (hole diameter = 10 mm).

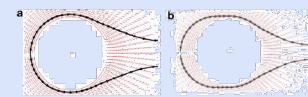


Fig. 8. Modification of fiber steering patterns: (a) FEA (1) trajectory and (b) (1) shifted 5 mm away from edge.

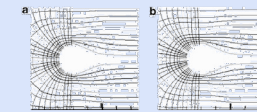


Fig. 9. Reduction of fiber over stacking: (a) FEA pattern and (b) modified pattern.



Fig. 16. Dimension of specimens.

Table 2 Boring test results					
Group	Ultimate failure mode	Peak load (kN)	Ultimate strength (MPa)	Weight (g)	Boring area (mm ²)
Baseline	Boring [12]	9.55	367.80	42.50	26.40
Steered	Net section [14]	22.16	441.28	61.75	24.80
Modified steered	Net section [14]	25.65	506.40	56.38	31.27

2016

Zur Erlangung des akademischen Grades
Doktor der Ingenieurwissenschaften
der Fakultät für Maschinenbau
Karlsruher Institut für Technologie (KIT)

Die orthotrope Wärmeleitung als numerischer Integrator
allgemeiner Richtungsfelder mit Anwendung zur optimalen
Faserplatzierung und Kraftflussvisualisierung

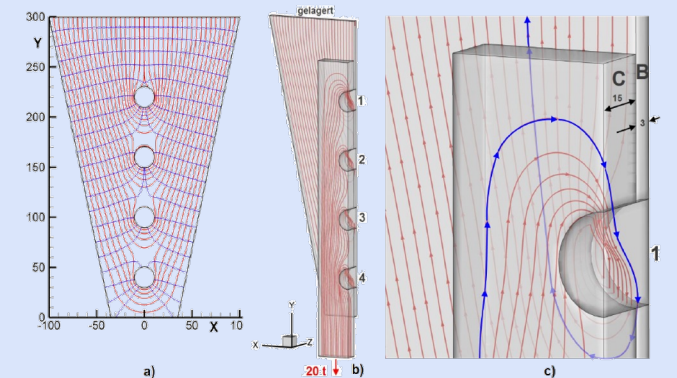
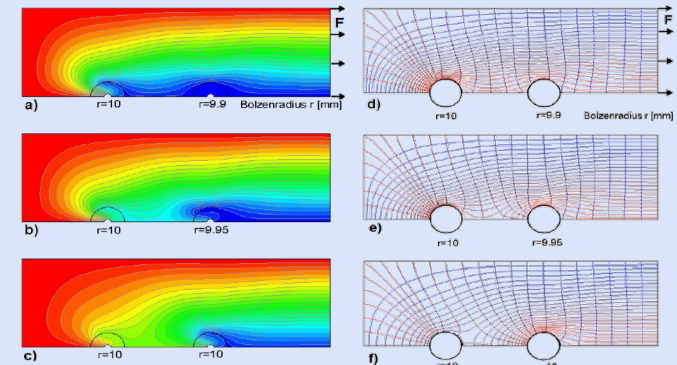
geneigte
Dissertation
von
Dipl.-Ing. Herbert Mollenhauer

Tag der Einreichung: 21. Juni 2016
Tag der mündlichen Prüfung: 12. September 2016

Hauptreferent: Prof. Dr. rer. nat. Claus Mattheck
Korreferent: Prof. Dr.-Ing. Frank Henning

Inhabere
Arbeits-Mattheck

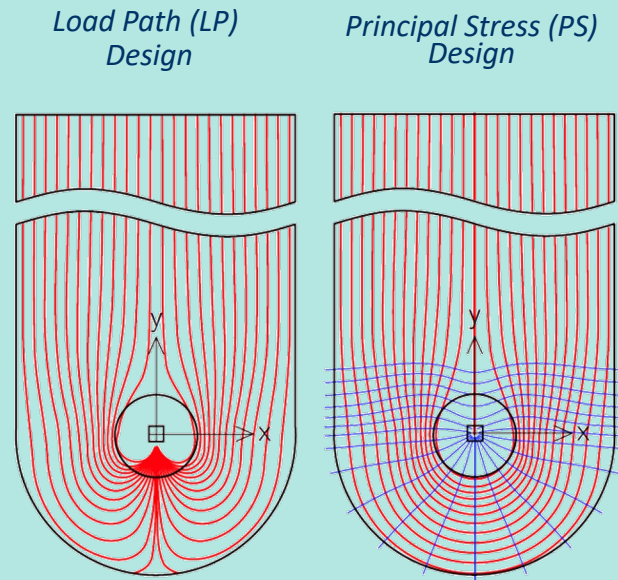
Die Visualisierung des Kraftflusses
in Stahlbaukonstruktionen



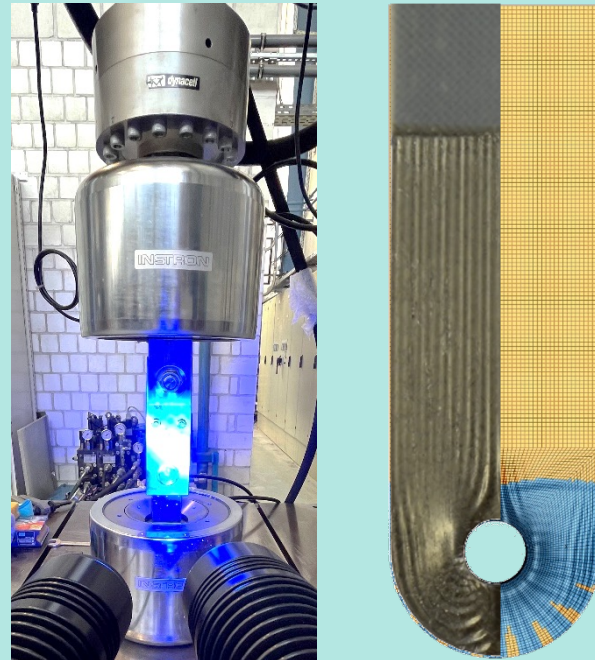
Bolted joints with tailored fiber orientation

Steps for optimizing design process

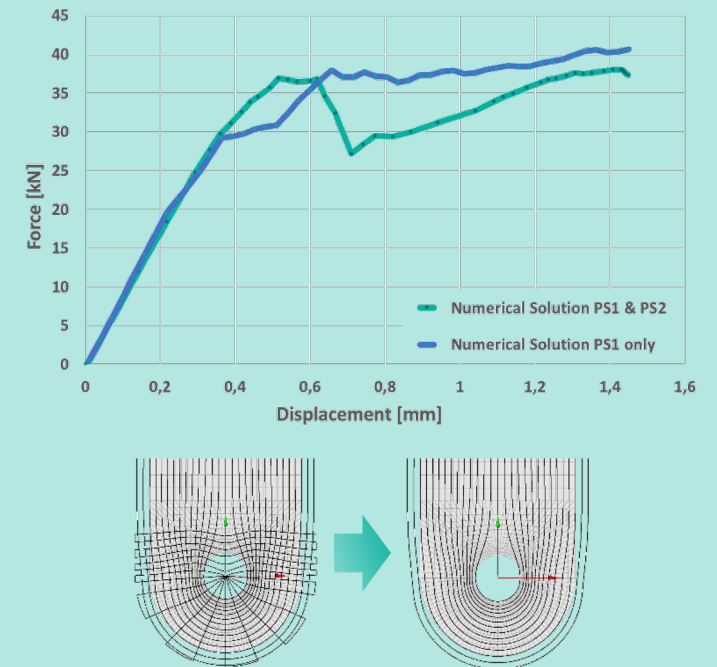
VA patter design based on isotropic calculations



Experimental evaluation and model calibration

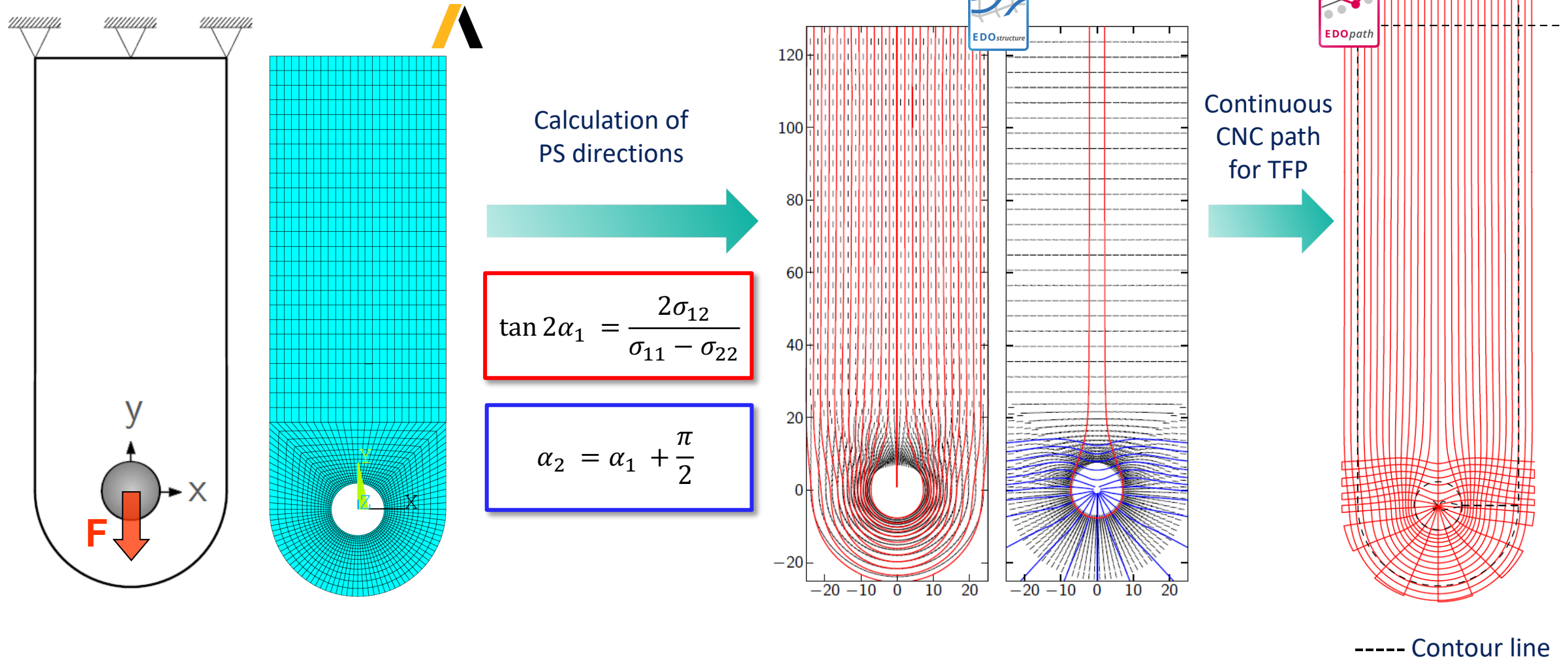


Optimization of VA pattern design



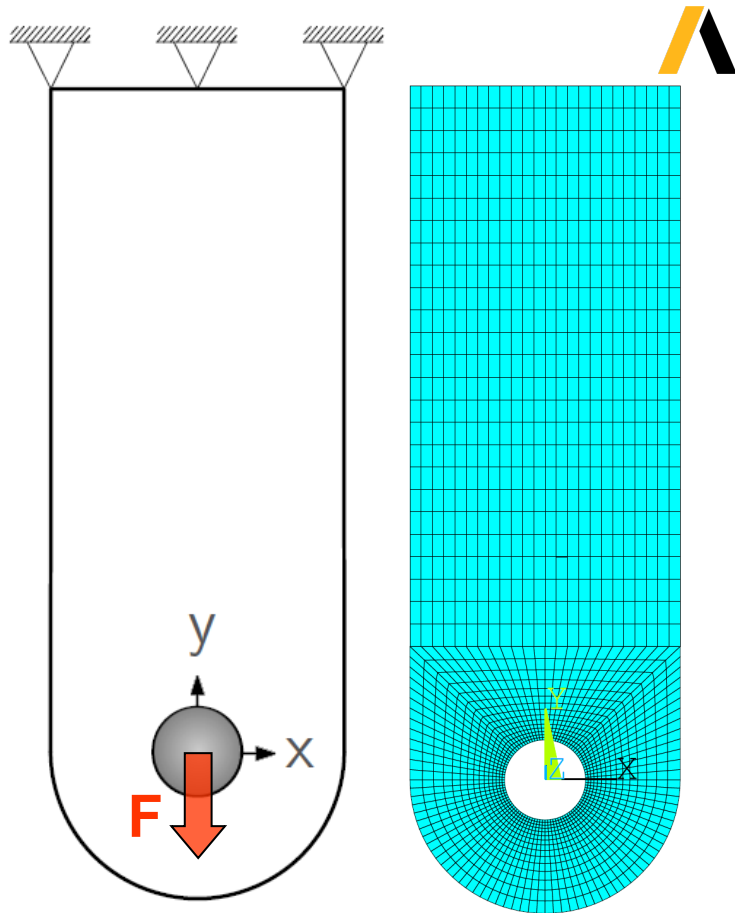
VA pattern design based on isotropic calculations

Principal Stress (PS) Design



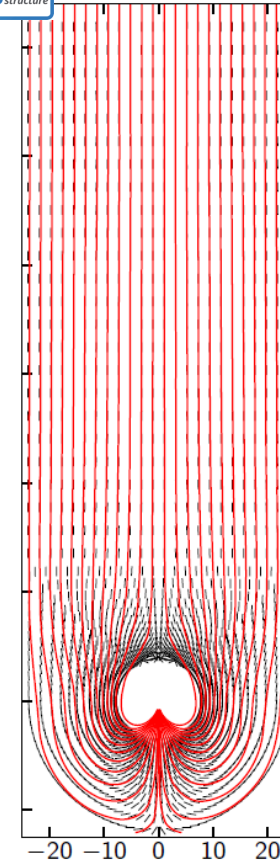
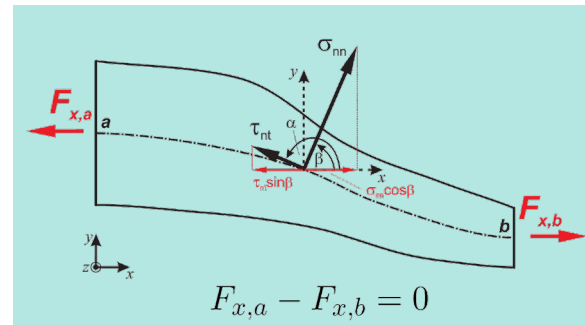
VA pattern design based on isotropic calculations

Load Path (LP) Design [1]

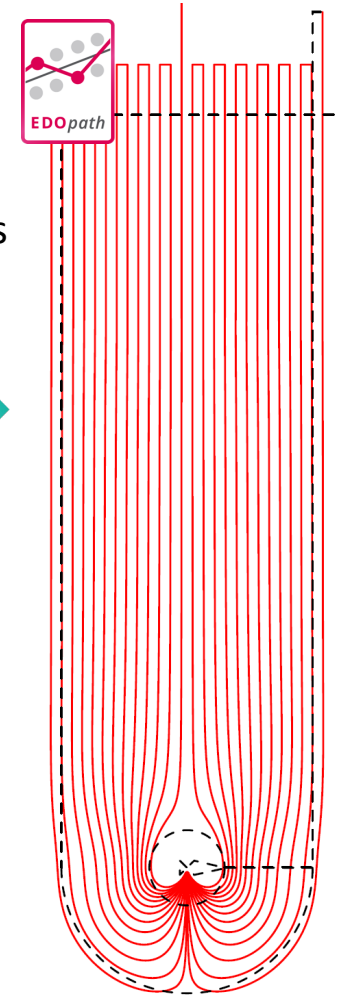


Calculation of
Load Path directions

$$\tan \alpha_y = \frac{\sigma_{12}}{\sigma_{11}}$$



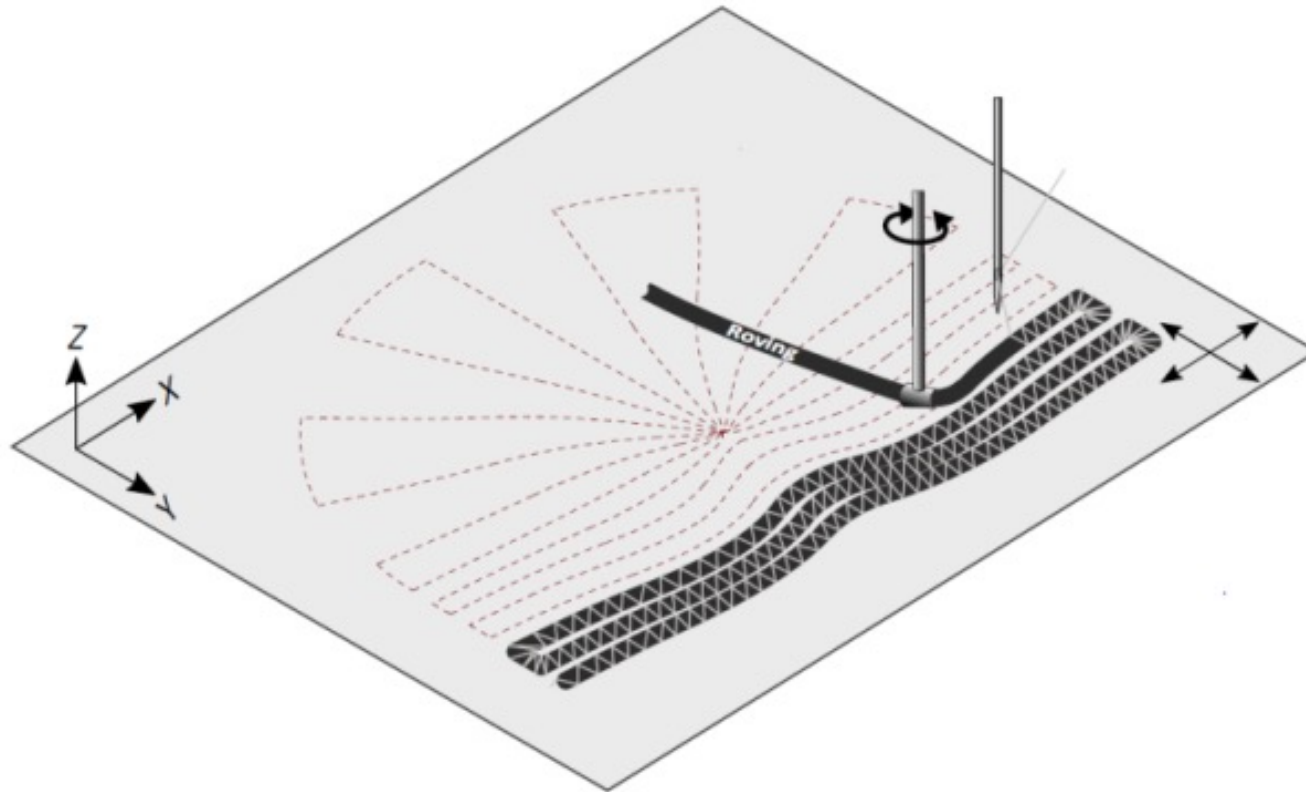
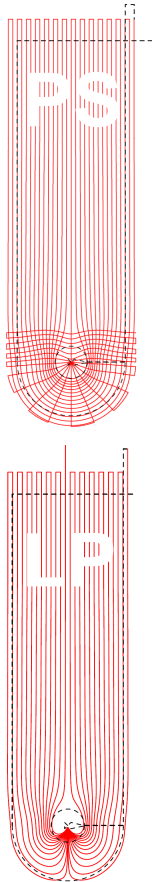
Continuous
CNC path
for TFP



----- Contour line

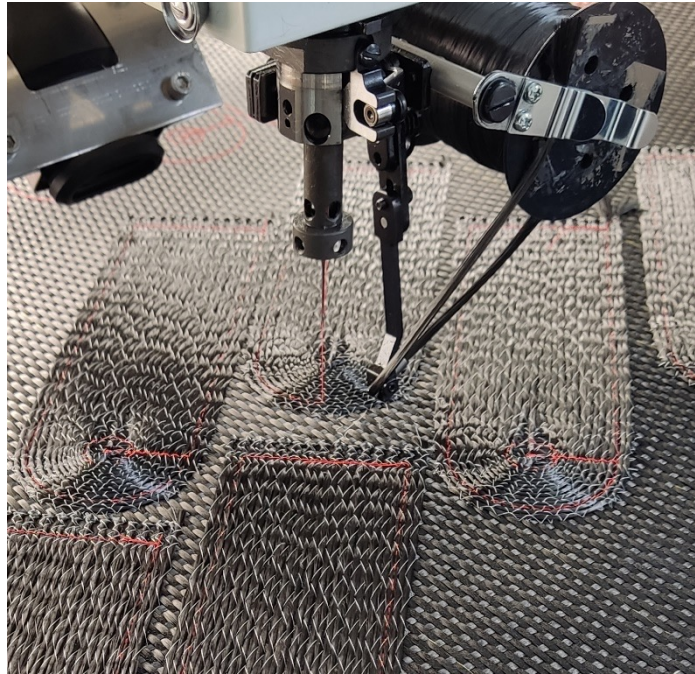
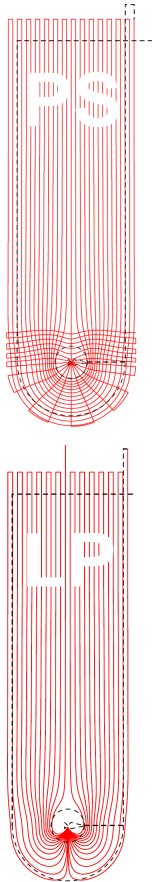
Experimental evaluation and model calibration

Manufacturing of specimen



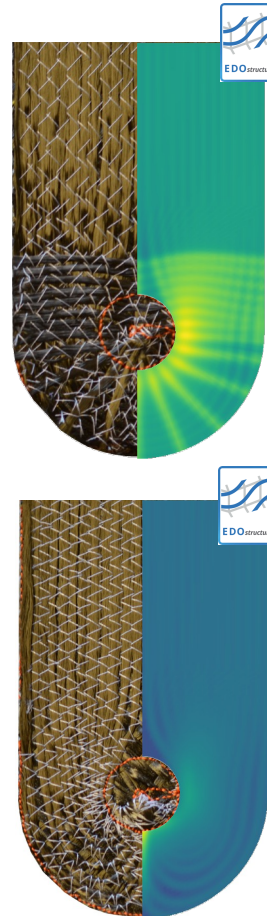
Experimental evaluation and model calibration

Manufacturing of specimen



Roving material: CF-HT, 400 tex (6k)

Base material: CF-HT woven fabric,
 $m_A = 380 \text{ g/m}^2$



Thickness
adapted
RTM molds



Epoxy resin: L20 + EPH 161

Experimental evaluation and model calibration

Specimen specification and experimental setup [2]



QI
 $m = 74 \text{ g}$
(base line)

[0/90/±45]_{4S}
(base material only)



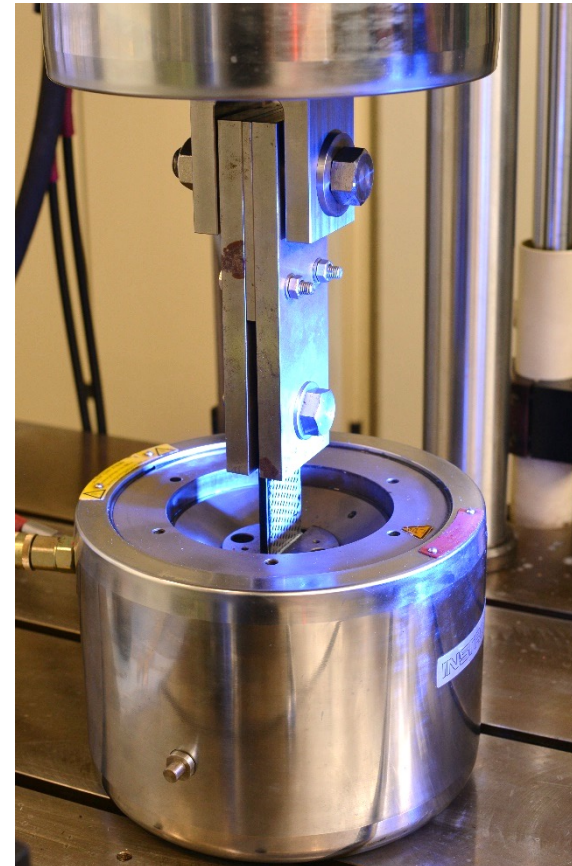
LP
 $m = 59 \text{ g}$

[LP/±45]_{4S}



PS
 $m = 57 \text{ g}$

[PS2/PS1/±45]_{4S}



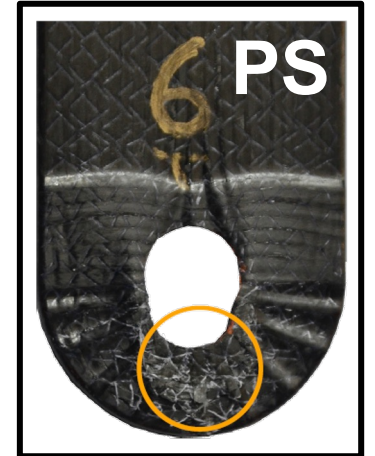
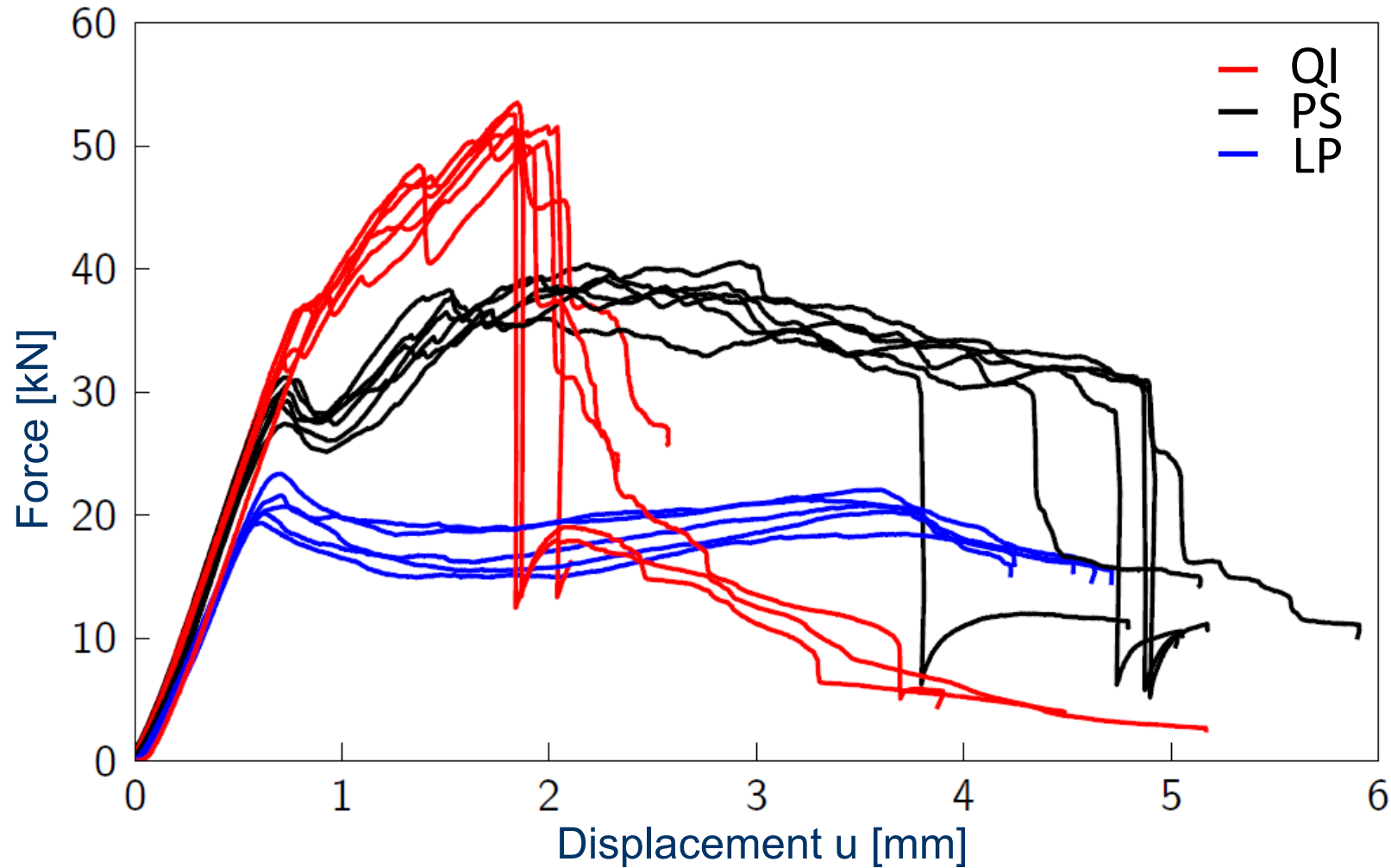
Test setup

- Instron 8088 with hydraulic clamping
- 250 kN load cell
- Preload: 50 N
- Test speed 1 mm/min
- Number of specimens: 6

Variable-axial specimens are about 22 % lighter than QI type

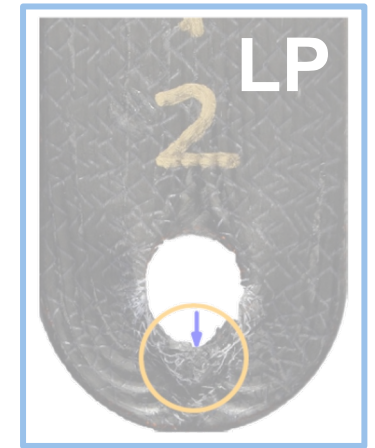
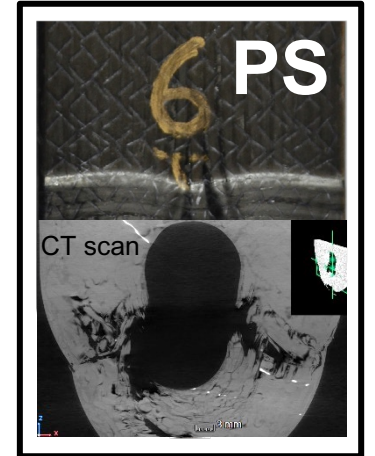
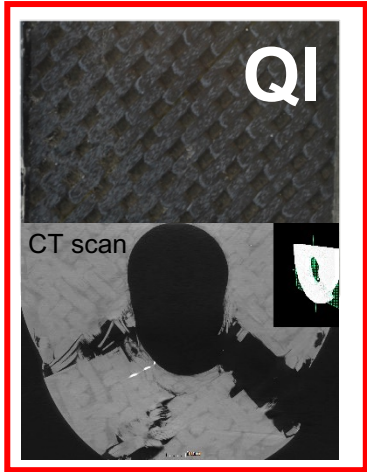
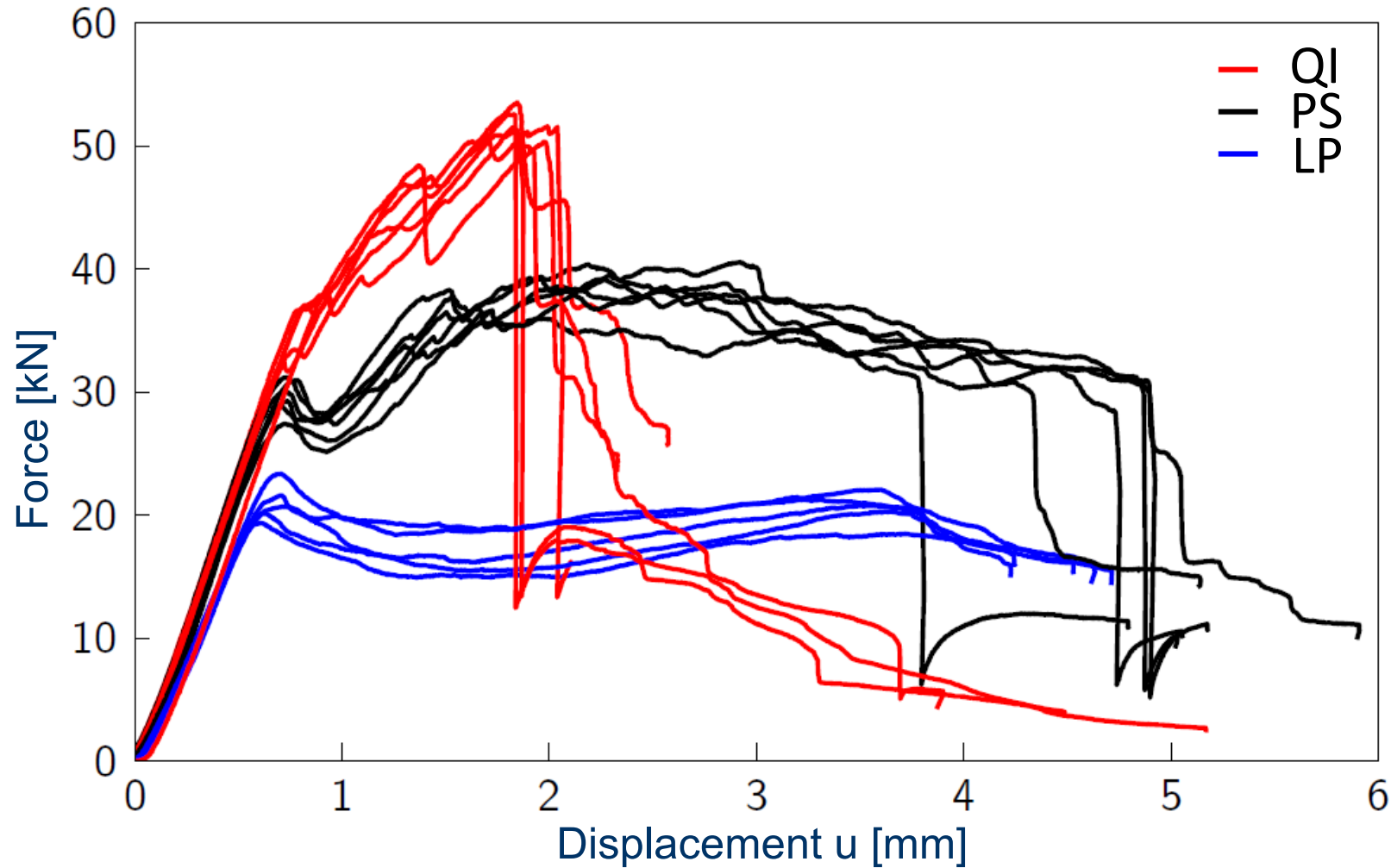
Experimental evaluation and model calibration

Results: Tensile test force-displacement diagram



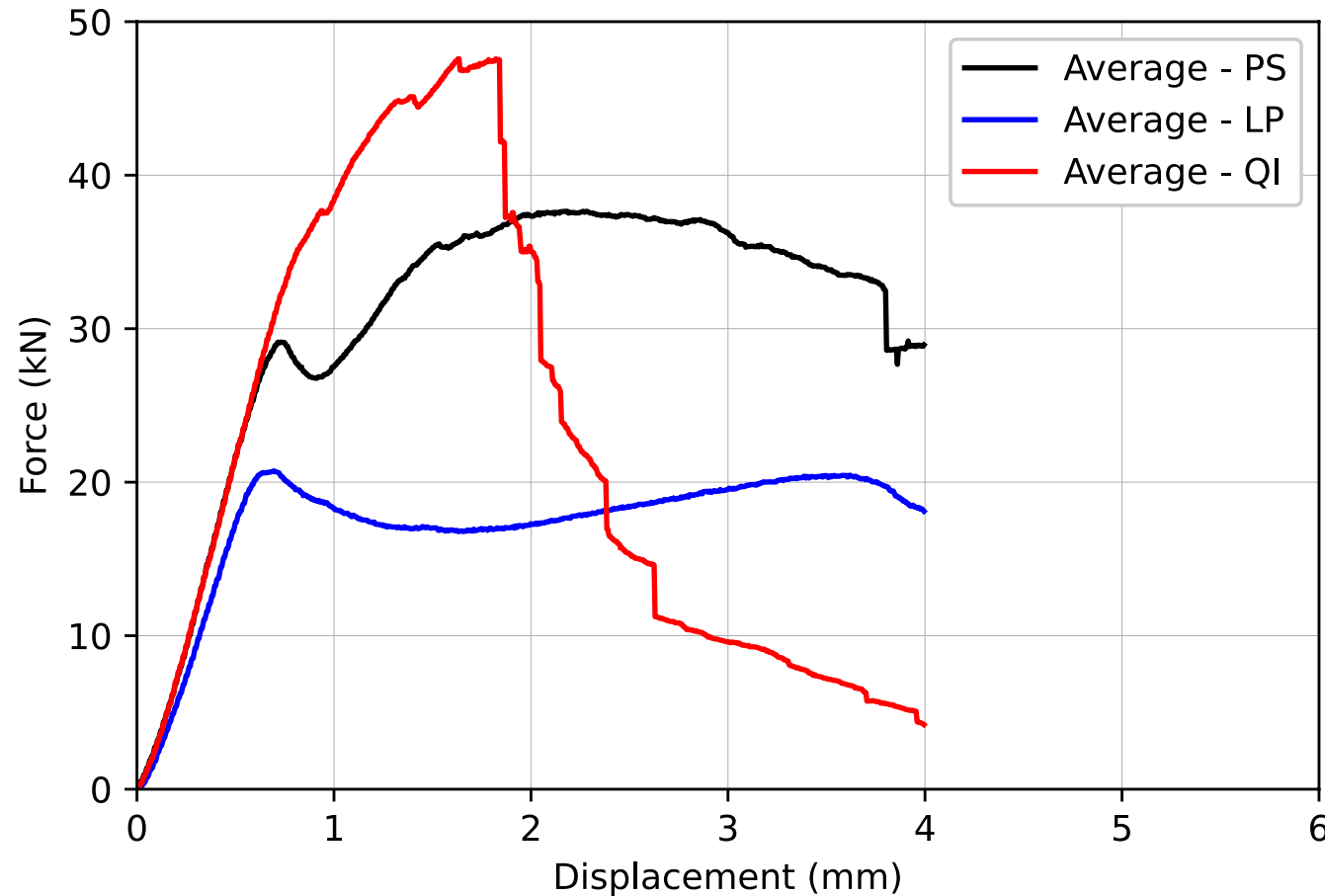
Experimental evaluation and model calibration

Results: Tensile test force-displacement diagram

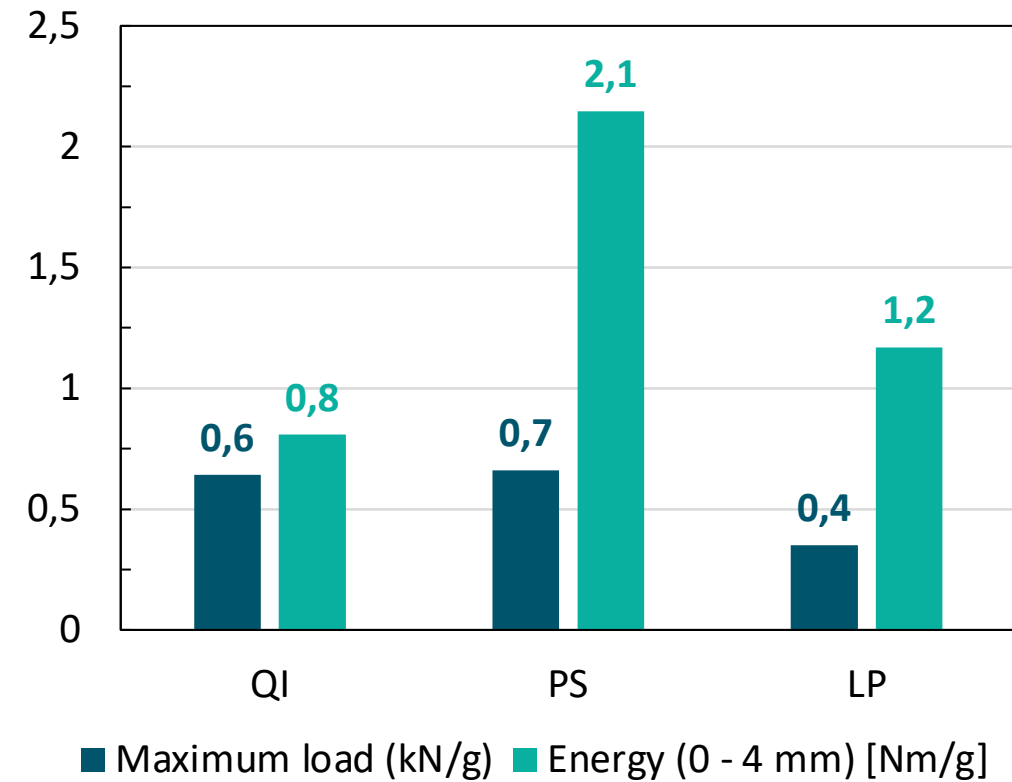


Experimental evaluation and model calibration

Results: Quasi-plastic deformation energy

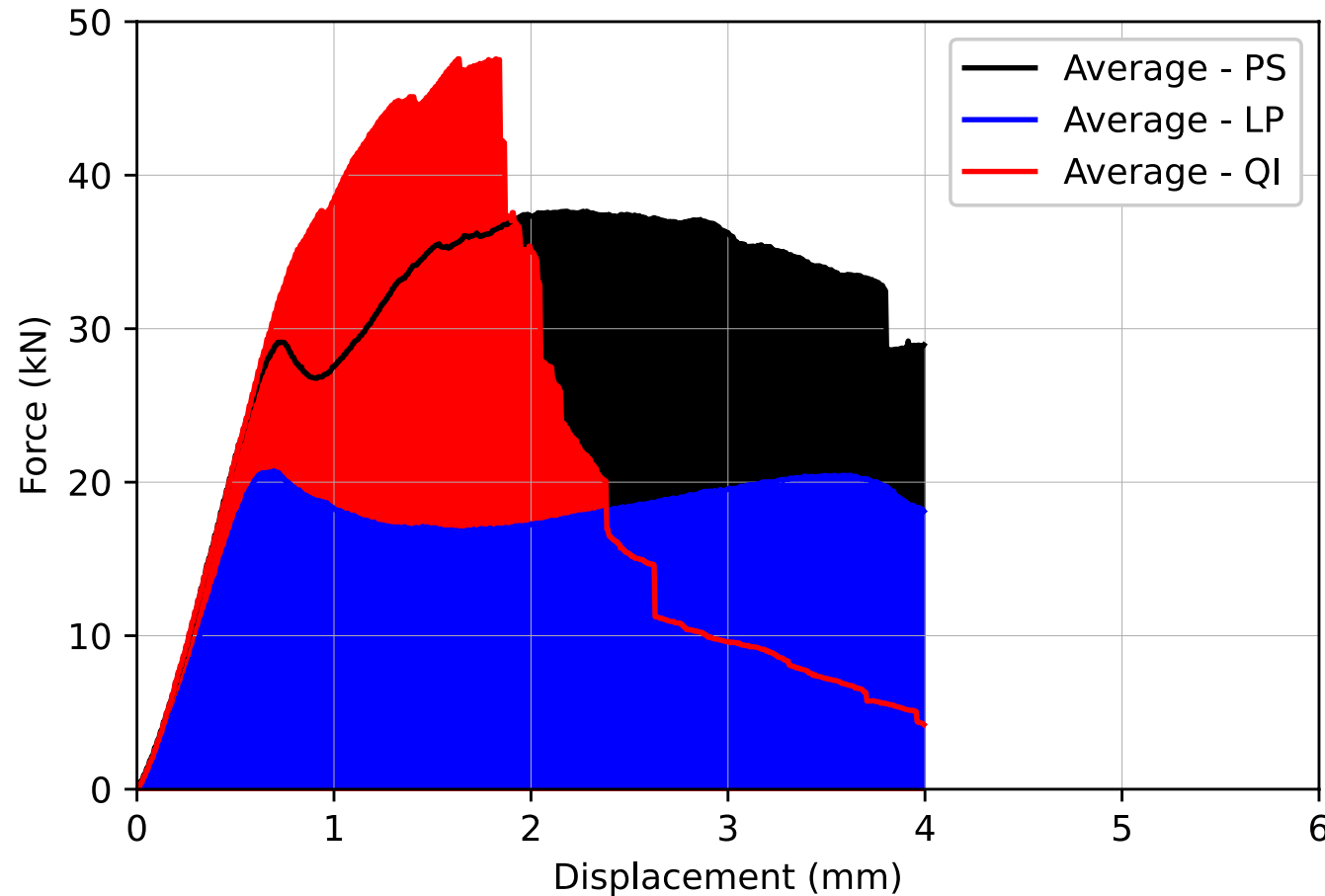


Mass-specific values

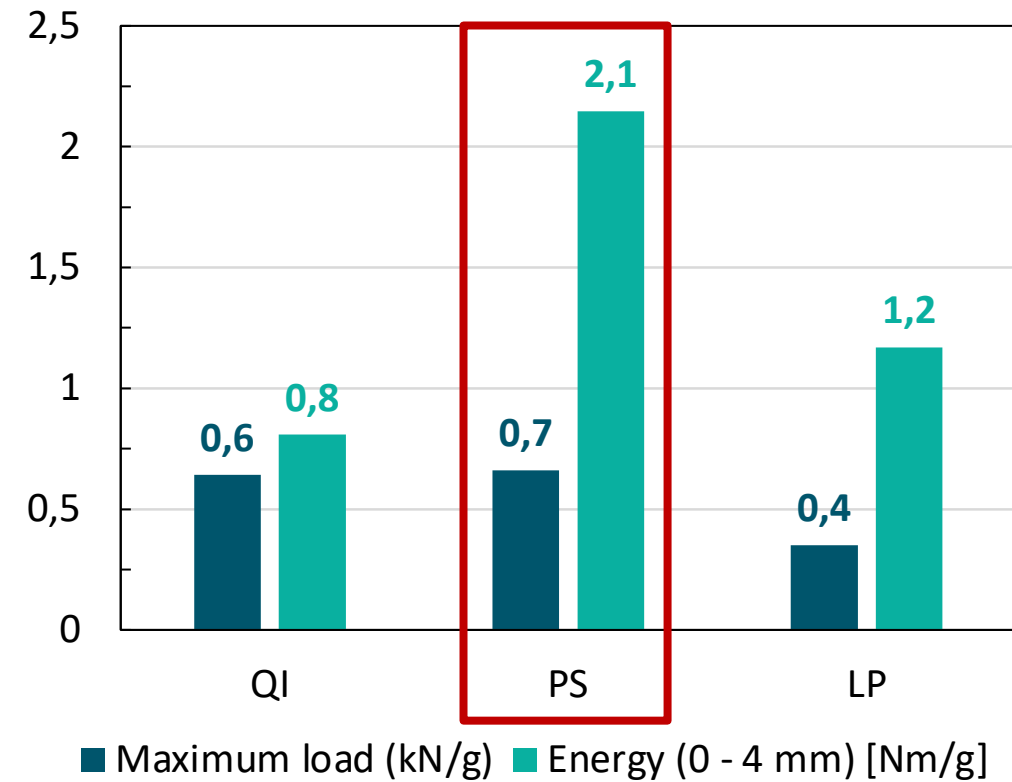


Experimental evaluation and model calibration

Results: Quasi-plastic deformation energy

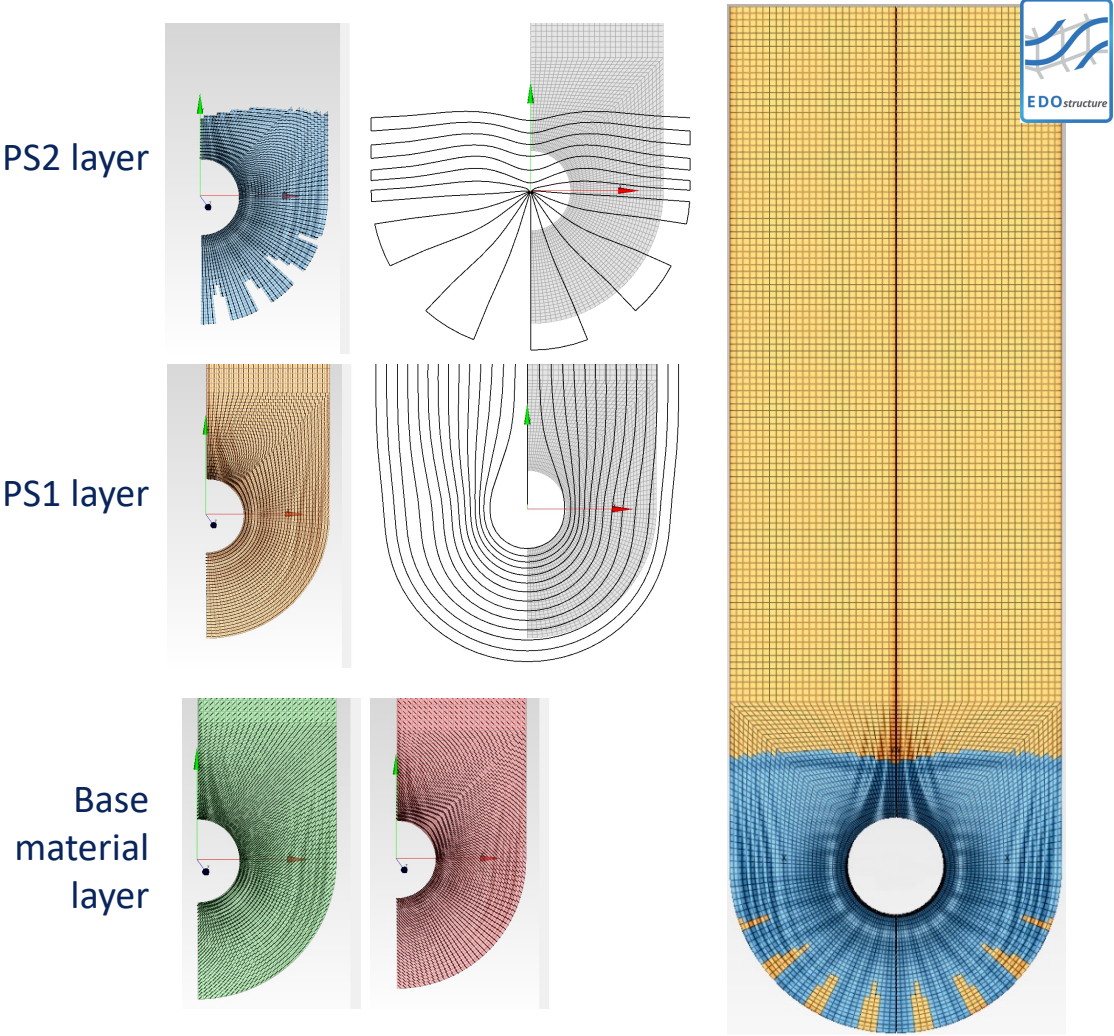


Mass-specific values



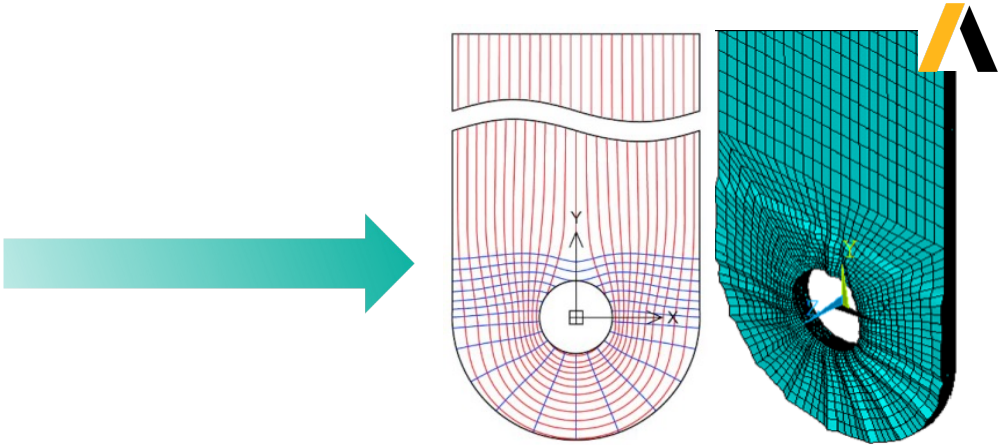
Model calibration

FE-modelling and material parameters



Numerical material parameters ($\phi = 55 \%$)

Fiber, Matrix	Composite
$E_{\parallel,f} = 238,000 \text{ MPa}$	$\sigma_{\parallel,t} = 1,409 \text{ MPa}$
$E_{\perp,f} = 16,000 \text{ MPa}$	$\sigma_{\parallel,c} = -7,40 \text{ MPa}$
$G_{\perp,f} = 50,000 \text{ MPa}$	$\sigma_{\perp,t} = 80 \text{ MPa}$
$\nu_{\perp,\parallel,f} = 0.27$	$\sigma_{\perp,c} = -140 \text{ MPa}$
$E_M = 3,150 \text{ MPa}$	$\tau_{\perp\parallel} = \tau_{\perp\perp} = 69 \text{ MPa}$
$G_M = 1,150 \text{ MPa}$	
$\nu_M = 0.37$	



Model calibration

Progressive damage simulation with parameter identification by FEMU



HASHIN Failure Criterion [3]

$$\begin{aligned}
 &\text{Fiber} \quad \begin{cases} X_{FT} = \left(\frac{\sigma_{11}}{F_{1T}} \right)^2 + \left(\frac{\sigma_{12}^2 + \sigma_{13}^2}{F_6} \right) & \sigma_{11} \geq 0 \\ X_{FC} = \left(\frac{\sigma_{11}}{F_{1C}} \right)^2 & \sigma_{11} < 0 \end{cases} \\
 &\text{Matrix} \quad \begin{cases} X_{MT} = \left(\frac{\sigma_{22}}{F_{2T}} \right)^2 + \left(\frac{\sigma_{23}}{F_4} \right)^2 + \frac{\sigma_{12}^2 + \sigma_{13}^2}{F_6^2} & \sigma_{22} \geq 0 \\ X_{MC} = \frac{\sigma_{22}}{F_{2C}} \left[\left(\frac{F_{2C}}{2F_4} \right)^2 - 1 \right] + \left(\frac{\sigma_{22}}{2F_4} \right)^2 \\ \quad + \left(\frac{\sigma_{23}}{F_4} \right)^2 + \frac{\sigma_{12}^2}{F_6^2} & \sigma_{22} < 0 \end{cases}
 \end{aligned}$$

Progressive damage modelling [3]

$$\mathbf{D} = \begin{bmatrix} \frac{C_{11}}{(1-d_f)} & C_{12} & C_{13} & 0 & 0 & 0 \\ C_{21} & \frac{C_{22}}{(1-d_m)} & C_{23} & 0 & 0 & 0 \\ C_{31} & C_{32} & \frac{C_{33}}{(1-d_m)} & 0 & 0 & 0 \\ 0 & 0 & 0 & \frac{C_{44}}{(1-d_s)} & 0 & 0 \\ 0 & 0 & 0 & 0 & \frac{C_{55}}{(1-d_s)} & 0 \\ 0 & 0 & 0 & 0 & 0 & \frac{C_{66}}{(1-d_s)} \end{bmatrix}^{-1}$$

$$d_f = \begin{cases} d_{ft} & \sigma_{11} \geq 0 \\ d_{fc} & \sigma_{11} < 0 \end{cases} \quad d_m = \begin{cases} d_{mt} & \sigma_{22} \geq 0 \\ d_{mc} & \sigma_{22} < 0 \end{cases}$$

$$d_s = 1 - (1 - d_{ft}) (1 - d_{fc}) (1 - d_{mt}) (1 - d_{mc})$$

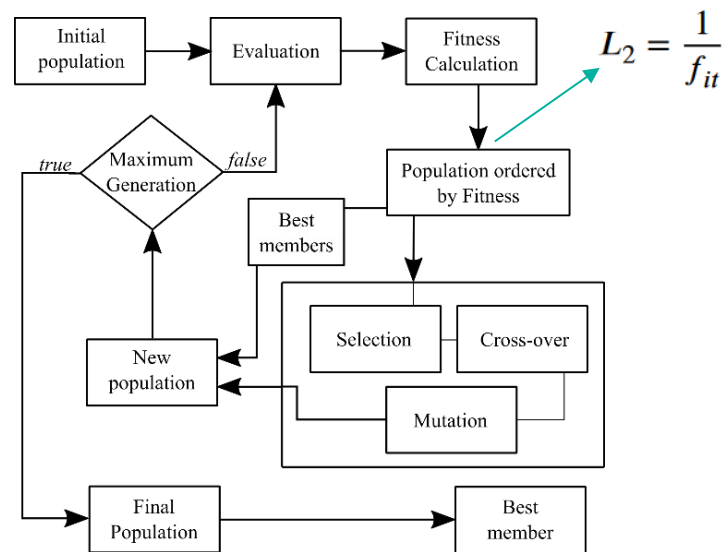
Model calibration

Progressive damage simulation with parameter identification by FEMU

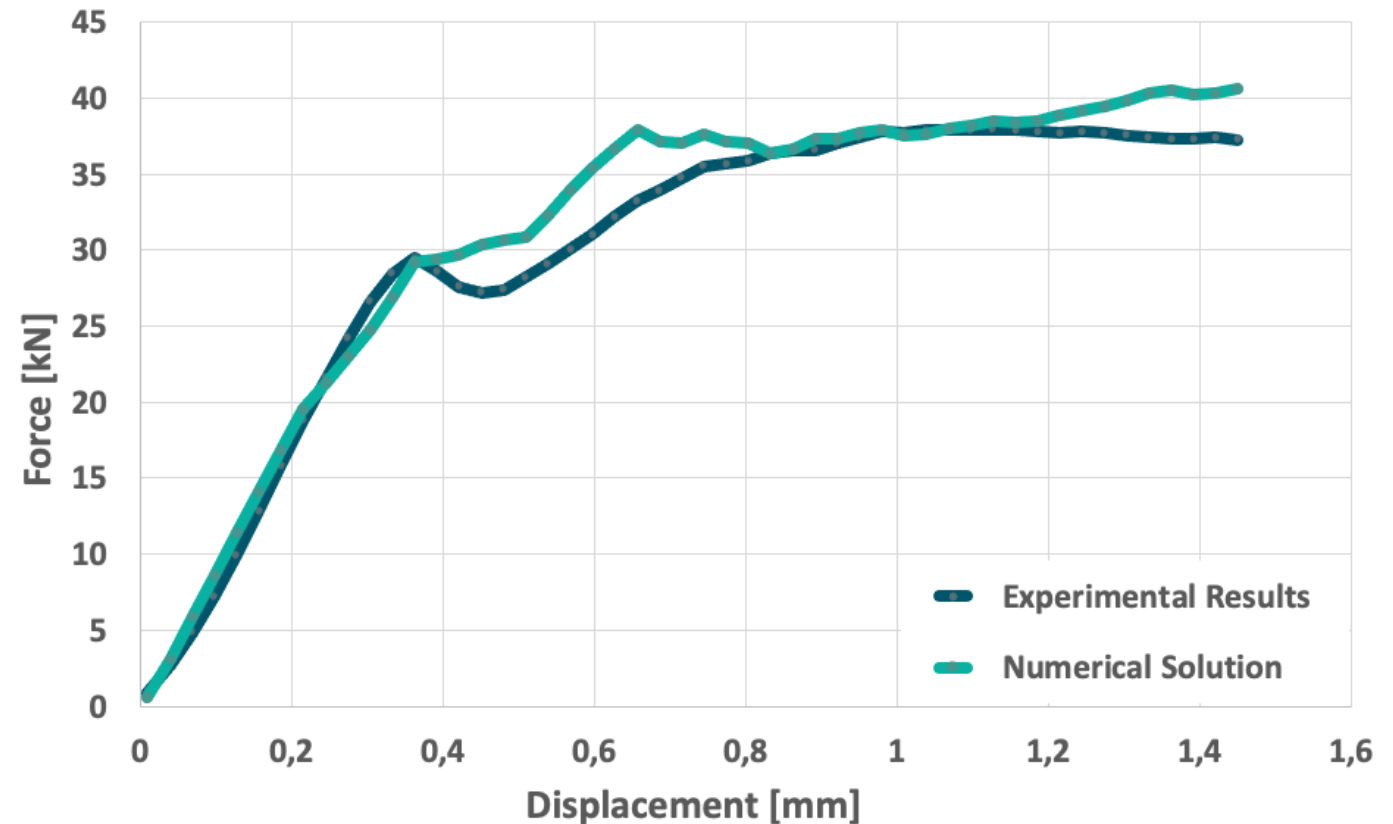
Stiffness degradation parameters [4] $\rho = \{d_{ft} \quad d_{fc} \quad d_{mt} \quad d_{mc}\}$

$$\min_{\rho \in [0,1]} L_2(\rho) = \min_{\rho \in [0,1]} \frac{1}{n_{ptos}} \sqrt{\sum_{i=1}^{n_{ptos}} \left(\frac{y_i^E - y_i^N(\rho)}{y_i^E} \right)^2}$$

Genetic Algorithm-based [4]



PS Design – Comparison exp. vs. num. results



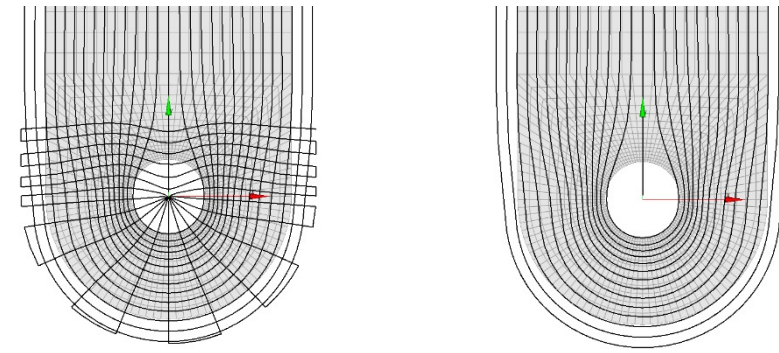
Conclusion and Outlook

Bolt joint loaded composites with a variable-axial fiber design shows improved quasi-plastic behavior compared to QI multi-axial laminate.

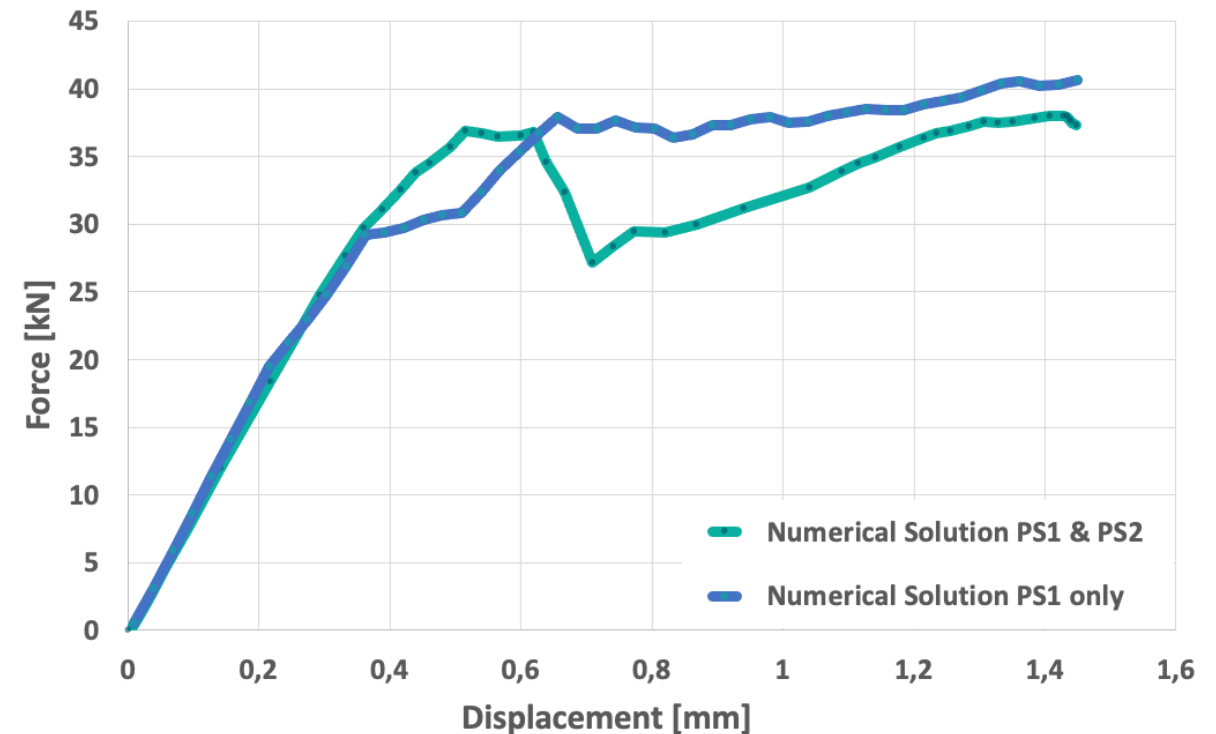
- Optimality based PS design shows higher mass energy absorption than LP design
- By help of experimental tests a progressive damage modelling setup was identified

Optimization of variable-axial fiber patterns by using, e.g., DFPO [5]

- Optimizing for maximal mass-specific loads
- Optimizing for even higher energy absorption



Comparison PS1+PS2 vs. PS1 only pattern specimen



Contact

Prof. Dr.-Ing. Axel Spickenheuer

Leibniz-Institut für Polymerforschung Dresden e. V.

Phone: +49 351 4658 374

E-Mail: spickenheuer@ipfdd.de

Web: www.ipfdd.de/tfp-technology



Research group *Complex Structural Components*

Acknowledgement

Karthick Selvaraj, Nicole Schmidt,
Falk Hähnel, Gustavo de Abreu
Cáceres, and Leonardo Chiquita

Thank you for your attention